Computational Structures Technology
B.H.V. Topping and Z. Bittnar, (Editors)
Saxe-Coburg Publications, Stirling, Scotland, 1-31.

Chapter 1

On the Finite Element Analysis of Shells and their Full Interaction with Navier-Stokes Fluid Flows

K.J. Bathe†, J.F. Hiller† and H. Zhang‡
† Department of Mechanical Engineering
Massachusetts Institute of Technology, Cambridge, Massachusetts, USA
‡ ADINA R&D, Inc.
Watertown, Massachusetts, USA

Abstract

Our objective is to present an overview of some of our latest research and developments in the finite element analysis of shells, Navier-Stokes fluid flows and the full interactions of these flows with general shell structures. In the area of shell analysis, we have studied some generic physical behaviours of shells with specific emphasis on boundary and internal layers as the thickness of the shell decreases. Furthermore, we have studied how best to evaluate general finite element discretization schemes when considering the variety of shell behaviours. We review in this paper some of the results obtained. In the area of fluid flow analysis, we are developing a new solution approach (a flow-condition-based interpolation, FCBI, finite element scheme) to solve high Reynolds number incompressible fluid flows. This scheme has a number of advantages as discussed and demonstrated in the paper. In particular, the procedure is useful for the solution of fluid flows fully coupled to shells and other structures.

Keywords: shells, asymptotic analyses, high Re flows, fluid-flow structural interactions, finite element solutions.

1 Introduction

Although the development of finite element methods for industrial and scientific analyses has been actively pursued for almost half a century, see e.g. [1], there are still major challenges in the field. Indeed, the possibilities for further advances and exciting applications are daunting and will provide for much further excitement in research and development [2,3].

Three areas of research that still require considerable developments are the analysis of general shell structures, the analysis of general Navier-Stokes fluid flows, and the solution of these flows fully coupled to shell structures.

The analysis of shell structures has been an active research field from the first developments of modern finite element methods. Indeed, it was the demand for more accurate analyses of shell aircraft structures that initiated to a large extent the development of finite element methods. However, although first analyses of complex shells were carried out already decades ago, the search for more accurate and efficient shell solution techniques has continued. The essence of these developments lies in establishing improved general shell finite elements and here the use of mixed methods has greatly advanced the field [1, 4]. At the same time as general shell finite element solution capabilities were developed, mathematical insights and theories have been established that greatly help in analysing and assessing finite element procedures [4-8]. Indeed, any finite element discretization technique that is now in use or newly proposed should really be evaluated using the current mathematical understanding. We review some of the important considerations regarding the assessment of shell discretization techniques in Section 2 of this paper.

With powerful finite element procedures now available, also more detailed numerical studies of shell structural behaviours can be pursued, in linear and nonlinear analyses. These studies, together with mathematical insight, have led to some very valuable understanding regarding boundary and internal layers in shells and the required meshing that accurately can resolve these layers. Shell structures need generally be designed to take account of such layers [9] and thus it is important to accurately assess the energy concentrations in these areas. We present in Section 2 also briefly some shell analysis results showing boundary and internal layers.

Considering fluid flow predictions based on the solution of the Navier-Stokes (or Euler) equations, much research has been performed over the last decades to develop finite element methods. Nevertheless, finite element techniques are not extensively used in engineering practice and instead finite volume methods are employed widely, see e.g. [2]. There are two major reasons. Firstly, finite volume methods have the advantage that local conservation of mass and momentum is satisfied in the traditional sense. This conservation property is of great importance in flow solutions, and traditional finite element methods only satisfy "flux equilibrium" on the nodal levels (as force equilibrium in structural analysis) [1]. Secondly, the traditional finite element methods have difficulties to converge in high Reynolds number flow solutions. A study to assess finite element methods in this respect was presented in reference [10].

The finite volume methods have of course also shortcomings. In particular, since interpolation functions are not explicitly employed, derivatives of the governing vector equations are difficult to establish and hence consistent Newton-Raphson solution schemes are hardly used. This leads to many iterations in order to reach solutions and presents difficulties, in particular in the analysis of fluid flow structural interaction problems where consistent Newton-Raphson iterations need be employed. Also, of course, as in finite element methods, artificial stabilization parameters are frequently used.

We are focusing on the development of a new finite element approach to reach a solution scheme closer to the "ideal" solution method described in reference [10]. The new finite element scheme is based on flow-condition-based interpolations, and hence is referred to as an FCBI finite element scheme [11], satisfies mass and momentum conservation for the element control volumes used, gives reasonable solutions for even coarse finite element meshes, and can be used with consistent tangent matrices in the Newton-Raphson iterations. We review the FCBI scheme in Section 3 of the paper.

The methods that we have developed for the solution of the Navier-Stokes equations governing compressible and incompressible fluid flows fully coupled with structural response have been employed successfully in the industrial environment for some years. The solution of such problems is based on the use of an arbitrary Lagrangian-Eulerian solution scheme and completely different meshes for the structures and fluids [12-17]. The FCBI finite element procedure, developed for incompressible flow simulations, enhances the effectiveness of the finite element solution of complex fluid flow structural interaction problems. We briefly demonstrate the use of the solution scheme for such problems in Section 4.

Finally, we conclude the presentation in Section 5 with some remarks regarding future developments. Of course, significant further advances are still much needed in discretization techniques for shells and fluid flows. For these developments we can build upon the methods reviewed here. In addition, we point out that there are major related areas of research that will provide challenges for many years to come.

2 On the physical behaviour of shells and the assessment of finite element discretization procedures

Our objective in this section is to briefly focus on the physical behaviour of shell structures with the mathematical characterization thereof, and then comment on the proper testing of discretization schemes.

2.1 Mathematical characterization of shell behaviours

Shell structural problems have been for a long time classified as membrane-dominated, bending-dominated and mixed problems. This classification can be made particularly precise by considering the asymptotic behaviours of shells [4,5,18,19].

Consider a shell mathematical model governed by equations that in variational form result in the problem statement [4,5]

$$\begin{aligned} &\textit{Find } u^{\varepsilon} \in V \textit{ such that} \\ &\varepsilon^3 A_b(u^{\varepsilon}, v) + \varepsilon A_m(u^{\varepsilon}, v) = \varepsilon^{\rho} G(v), \quad \forall v \in V \end{aligned} \tag{1}$$

where $\varepsilon = t/L$, t is the thickness and L is a global characteristic dimension of the shell structure, the bilinear form A_b represents the scaled bending energy, the bilinear form A_m represents the scaled membrane and shear energies, u^{ε} is the unknown solution (displacement field), v is the test function, V is the appropriate Sobolev space, and G denotes the scaled external loading. It can be proven that, when a well-defined scaling exists, we have $1 \le \rho \le 3$.

The following subspace plays a crucial role in characterizing the asymptotic behaviour of a shell as ε approaches zero [5]

$$V_0 = \{ v \in V \mid A_m(v, v) = 0 \}. \tag{2}$$

If the content of this pure-bending subspace is only the zero displacement field ($V_0 = \{0\}$), we say that "pure bending is inhibited" (or, in short, we have an "inhibited shell"). On the other hand, when the shell admits nonzero pure-bending displacements, we say that "pure bending is non-inhibited" (we have a "non-inhibited shell"). The classification of shells into the different fundamental behaviours highly depends on whether the shell is inhibited or not.

In case pure bending is non-inhibited (that is, $V_0 \neq \{0\}$), frequently the bending-dominated state is reached and the appropriate value to use for the load-scaling factor ρ is 3. The general form of the limit problem is

$$\begin{aligned} &\textit{Find } u^0 \in V_0 \textit{ such that} \\ &A_b(u^0, v) = G(v), \quad \forall v \in V_0. \end{aligned} \tag{3}$$

Of course, this limit problem holds only when the loading activates the pure bending displacements; otherwise, the shell behaviour is as for the inhibited case but unstable [4,5].

In case pure bending is inhibited (that is, $V_0 = \{0\}$), we use the load-scaling factor $\rho = 1$. Then, provided the problem is well-posed, we obtain the limit problem of the membrane-dominated case in the space V_m, a space larger than V, consisting of all displacements of bounded membrane and shear energies only

$$\begin{aligned} &\textit{Find } u^m \in V_m \textit{ such that} \\ &A_m(u^m, v) = G(v), \forall v \in V_m. \end{aligned} \tag{4}$$

This problem is well-posed provided the loading G is in the dual space of V_m. The condition $G \in V_m'$ is directly equivalent to

$$|G(v)| \leq C\sqrt{A_m(v,v)}\,, \quad \forall v \in V \tag{5}$$

with C a constant. Equation (5) ensures that the applied loading can be resisted by membrane stresses only. If this is not possible, the asymptotic state does not correspond to membrane energy only, and the shell problem is classified as a mixed problem.

The asymptotic categories of shell behaviours are summarized in Table 1. In the further discussion we focus on the cases (i), (iii) and (iv). The unstable case (ii) is of course also in general of interest (see references [4,5] for examples) but is not of interest for the focus of our discussion given below, that is, for the proper testing of finite element procedures.

Various numerical schemes to calculate the load-scaling factor ρ have been discussed in reference [19], see also reference [20]. If a constant surface-distributed load is applied, we evaluate for decreasing values of ε

$$\overline{\rho} = -\frac{\log E(\varepsilon_1) - \log E(\varepsilon_2)}{\log \varepsilon_1 - \log \varepsilon_2} \tag{6}$$

where $E(\varepsilon_1)$ and $E(\varepsilon_2)$ are, respectively, the total strain energies corresponding to ε_1 and ε_2. Then we have

$$\rho = \lim_{\varepsilon_1, \varepsilon_2 \to 0} \overline{\rho}\ . \tag{7}$$

Using finite element solutions, the asymptotic behaviours of three shell problems were solved in reference [19], namely a hyperbolic paraboloid shell problem, the original Scordelis-Lo roof problem and a modified Scordelis-Lo roof problem. These problems are, respectively, a bending-dominated, mixed, and membrane-dominated problem and in each case a well-defined load-scaling factor was computed. Of course, there are also shell problems that do not show a well-defined load-scaling factor, and in reference [20] we present and analyse such a problem (colloquially referred to as a "monster shell problem").

The various physical behaviours of shell structures that can be reached are most interesting. In particular, the boundary and internal layers in shell structures provide for complex behaviours. Figures 1 and 2 show some shell structural analysis results where boundary and internal layers can be seen. When assessing finite element solution procedures, particular attention must be given to such layers as further discussed in the following section.

Case	Loading	Category
Non-inhibited shell $V_0 \neq \{0\}$	Loading activates pure bending displacements $\exists v \in V_0$ *such that* $G(v) \neq 0$	(i) Bending dominated
	Loading does not activate pure bending displacements $G(v) = 0\,,\ \forall v \in V_0$	(ii) Membrane dominated or mixed but unstable
Inhibited shell $V_0 = \{0\}$	Admissible membrane loading $G \in V_m'$	(iii) Membrane dominated
	Non-admissible membrane loading $G \notin V_m'$	(iv) Mixed

Table 1. The classification of shell asymptotic behaviours [19, 20].

2.2 Measuring errors in finite element discretization schemes

Shell finite element analyses have of course been performed for decades, and acceptable solutions in terms of some error assessment have been obtained. However, with advances in technology, more stringent requirements on shell solutions have evolved and accurate analyses of general shells need be performed routinely, in linear and nonlinear solutions.

The analysis of general shells is difficult because of the different behaviours that can be encountered, as summarized in the previous section. The shell finite element method should ideally be able to represent in a **uniformly** effective manner the behaviours in membrane, bending and mixed states, and should of course also be applicable to "monster shells". This is extremely difficult to achieve, and it has been recognized some time ago that a mixed formulation must be used. In this mixed formulation we should aim to satisfy:

Ellipticity
Each finite element and the complete finite element discretization, when not supported, must always only contain the six physical zero eigenvalues, corresponding to the rigid body modes, and not any additional zero eigenvalues which would be spurious (but of course, the finite elements and any assemblage thereof must also not contain less than the six physical zero eigenvalues). Many finite elements still in use violate this requirement and must be employed with great care. We cannot recommend the use of such elements for general shell analyses, see reference [1, p. 473].

Consistency
The discretization scheme must be "consistent" in representing all strain terms. This briefly means that the bilinear forms used in the finite element discretization, which are a function of the element size h, must approach the exact bilinear forms of the mathematical model as h goes to zero. Since the membrane and shear energy terms

are usually "weakened" in the finite element discretizations, in order to avoid "locking", the consistency errors in these terms must be controlled and should approach zero with the optimal order corresponding to the finite element interpolations used.

Inf-sup condition

Ideally, a mixed finite element scheme would satisfy the relevant inf-sup condition, see references [1, 4-8]. Shell elements that satisfy this condition are optimal in bending-dominated problems for the interpolations used. Hence, the elements would not lock and the error would be independent of the shell thickness. Unfortunately, no general shell element discretization scheme has so far been proven analytically to satisfy the inf-sup condition. So far only numerical tests have been performed on shell discretizations [7,8].

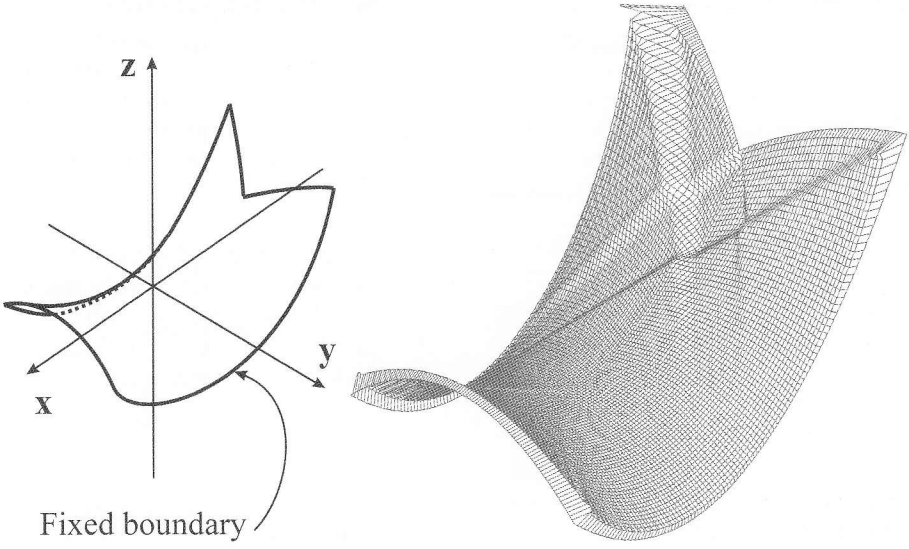

Figure 1. Deformation of the mid-surface of a shell showing boundary and internal layers. The equation of the mid-surface is given by

$$\begin{cases} z = (x^2 - y^2)/100 \\ |y| \le 50 \\ -75 - y/4 \le x \le 50 \quad when \quad 0 \le y \\ -75 + y/4 \le x \le 50 \quad when \quad y < 0 \end{cases}$$

and the shell is clamped along its edge. The thickness is $t = 0.00001$. The loading is a uniform force per unit area in the z direction applied over the entire structure. The numerical solution was obtained with MITC4 elements. Layers are clearly visible in the simulation results, both along the boundary and asymptotic lines.

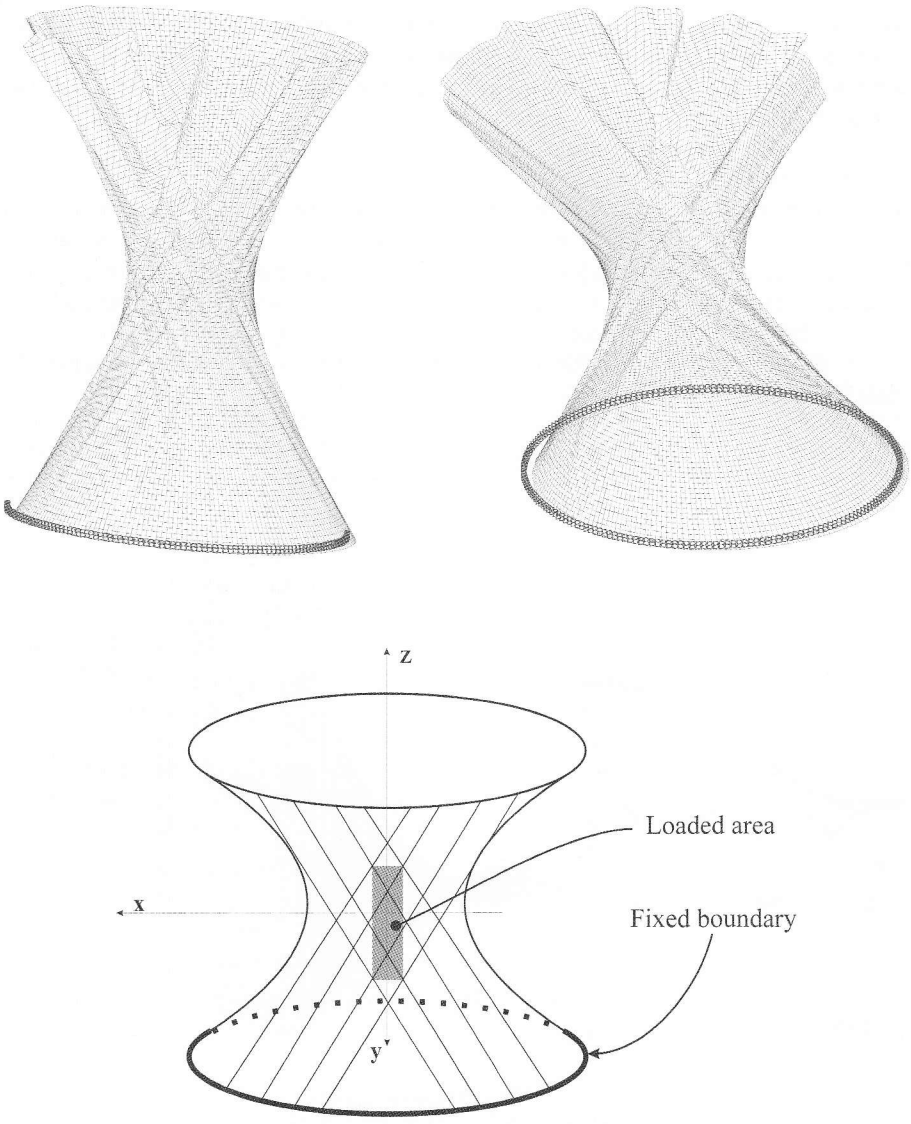

Figure 2. Deformation of the mid-surface of a shell showing internal layers. The mid-surface of the shell is an elliptic hyperboloid described by the equation $x^2/30 + y^2/10 = 1 + z^2/64$, $|z| \le 20$. The loading is a uniform force per unit area in the y direction, applied over the greyed area in the bottom figure. The shell is clamped along its bottom edge. The bottom figure also indicates the location of internal layers in the limit problem with zero thickness. In this problem the thickness is $t = 0.0001$.

Due to the complexity of shell behaviours, rigorous mathematical investigations on whether a shell discretization scheme is effective are still out of reach and therefore, largely, recourse to numerical investigations is necessary. However, these numerical studies need to be well-designed and based upon the general mathematical understanding already available.

The proper testing of a shell finite element discretization scheme should involve:

--- The analysis to see whether the ellipticity condition is satisfied. This is accomplished by simply ensuring that any generic single element does not contain a spurious zero energy mode.

--- The analysis of well-chosen shell problems to identify whether the consistency errors are under control, that is, these errors should diminish at the optimal rate. Since the shear and membrane bilinear forms are usually changed from those of the mathematical model, in order to avoid "locking", well-chosen membrane-dominated problems should be solved to see whether the exact solutions are reached and the optimal rates of convergence are obtained.

--- The analysis to see whether the inf-sup condition is satisfied. This analysis is the most difficult to perform. A complete analysis would include the inf-sup test of [7], in which the thickness of the shell does not enter, and the solution of well-designed bending-dominated problems to see whether the optimal rates of convergence are obtained. These convergence rates should always be independent of the shell thickness.

An important ingredient in solving the membrane- and bending-dominated problems is of course the use of an appropriate error measure. To assess displacement-based formulations, we would simply use

$$E(u,u_h) = A(u,u) - A(u_h,u_h) \tag{8}$$

where u and u_h denote the exact and the finite element solutions respectively and A is the energy operator. However, general shell elements are based on mixed formulations and, while this convergence measure can still be used, a more appropriate measure is

$$EM(u_{ref},u_h) = \frac{1}{2}\int_{\Omega} \Delta\varepsilon : C : \Delta\varepsilon \, d\Omega \tag{9}$$

(EM stands for "error measure") with $\Delta\varepsilon = \varepsilon_{ref} - \varepsilon_h$ where ε_{ref} denotes the reference strain tensor at a point (either an analytical solution or a very accurate numerical approximation thereof) and ε_h denotes the finite element strain tensor at the corresponding point of the mesh. Here C is the constitutive tensor and Ω the volume of the shell.

Another very important requirement in the convergence studies is to mesh the boundary and internal layers appropriately. Table 2 summarizes information on

layers and the thickness in each case encountered in shell analyses. To observe the actual and proper convergence rates of finite element discretizations, the meshing used should be such that the error (measured per unit volume or surface of the shell) is uniform in the finite element solutions [1].

To demonstrate these considerations in an analysis process, we consider the problem of the hyperboloid shell shown in Figure 3 solved using the MITC4 shell element. Of course, the MITC4 element satisfies the ellipticity condition. To numerically assess consistency, we consider the shell to be entirely fixed at both ends (due to the symmetries of the problem, we model only one eighth of the structure). The shell problem is then a well-posed membrane-dominated problem, with $\rho = 1$, see Table 3. Figure 4a shows the convergence curves obtained when uniform meshes are used for the solution. Note that, for each value of thickness of the shell, we consider increasingly finer uniform meshes. In these analyses, the boundary layer at the fixed edge did not receive any special treatment. The results show that, clearly, as the thickness of the shell decreases the convergence curves flatten out, indicating that the order of convergence is not uniformly optimal.

Relative thickness	Location of layer
$\varepsilon^{1/2}$	Along curves that are not characteristics
$\varepsilon^{1/3}$	Along characteristics of a hyperbolic geometry
$\varepsilon^{1/4}$	Along characteristics of a parabolic geometry

Table 2. Width of boundary and internal layers in shells.

Thickness	Clamped condition	Free condition
0.01	1.0465	2.99590
0.001	1.0134	2.99994
0.0001	1.0041	2.99998
0.00001	1.0013	NA
0.000001	1.0004	NA
0.0000001		

Table 3. Hyperboloid of revolution: values for $\overline{\rho}$ obtained by use of a very fine MITC16 element mesh.

Thickness	MITC4	QUAD9
t=0.01	0.53913610e3	0.5391545484e3
t=0.001	0.60002983e4	0.6000683733e4
t=0.0001	0.61878678e5	0.6189651974e5
t=0.00001	0.62436470e6	0.6248819710e6
t=0.000001	0.62566295e7	0.6267458173e7

Table 4. Strain energies in the clamped hyperboloid shell problem (one eighth modelled). Values were obtained with very fine graded meshes, with half of the elements located in the band near the clamped edge and half the elements located in the rest of the structure. For the MITC4 element, the mesh consisted of 192x192 elements, and for the displacement-based 9-node (QUAD9) element, the meshes consisted of 96x96 elements.

If on the other hand we next mesh the domain with proper care given to the boundary layer, using a uniform mesh over the band of width $6\sqrt{t}$ near the clamped edge and a uniform coarser mesh over the rest of the structure, we obtain the results shown in Figure 4b and we see that indeed for all values of shell thickness, practically, the optimal order of convergence is obtained. The curves are observed to shift slightly as the thickness decreases. Furthermore, the analysis results converge to the results obtained using the displacement-based formulation, as indicated in Table 4. As mentioned above, these results indicate that the consistency errors in the membrane/shear bilinear form are under control. Of course, when the thickness is very small, the mixed element can perform in the analysis of this problem only as well as the pure displacement-based 4-node element [5].

We now continue the experiment using the same shell geometry and loading but we consider the structure to be entirely free at its ends. This is a well-posed bending-dominated problem, with $\rho = 3$, see Table 3. The analysis results using graded meshes are shown in Figure 5. In this case as well, the optimal order of convergence is obtained, and the rate is independent of the thickness of the shell. Since there is no upwards shift in the convergence curves as the shell thickness is decreased, the element does not lock in this analysis. Hence, we would expect that the inf-sup condition is satisfied for this geometry and boundary conditions. These studies indicate that for these problems the MITC4 element performs in an optimal manner.

Of course, the above study is quite limited but clearly shows the importance of meshing boundary layers appropriately. Additional results that we have obtained regarding the limit behaviour analysis of shells and the testing of shell finite element discretizations are given in references [4-7,19-21].

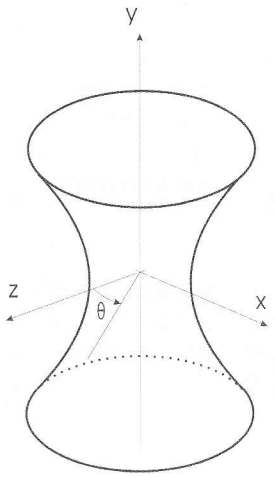

Figure 3. Hyperboloid shell geometry. The mid-surface is described by the equation (hyperboloid of one sheet) $x^2 + z^2 = 1 + y^2$. The loading used is a pressure of magnitude $p(\theta) = p_0 \cos(2\theta)$.

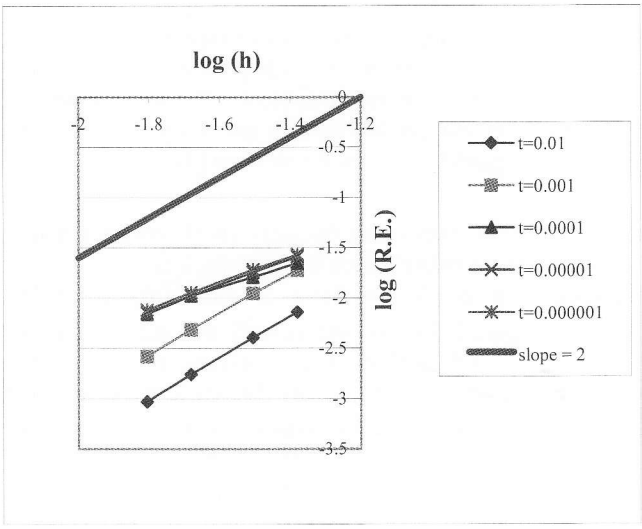

Figure 4a. Convergence curves for the clamped hyperboloid shell modelled with uniform meshes: we plot **log**(*R.E.*) where *R.E.* denotes the relative error $EM(u_{ref}, u_h) / A(u_{ref}, u_{ref})$ versus **log**(h).

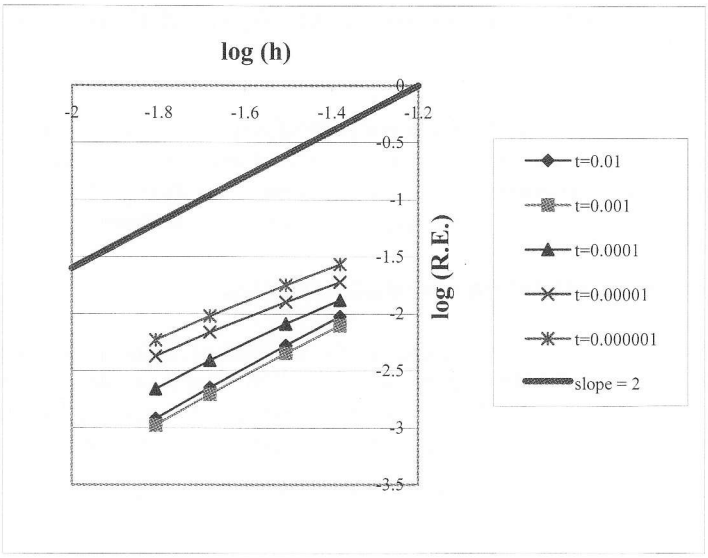

Figure 4b. Convergence curves for the clamped hyperboloid shell modelled with graded meshes: we plot **log**(*R.E.*) where *R.E.* denotes the relative error $EM(u_{ref}, u_h) / A(u_{ref}, u_{ref})$ versus **log**(h).

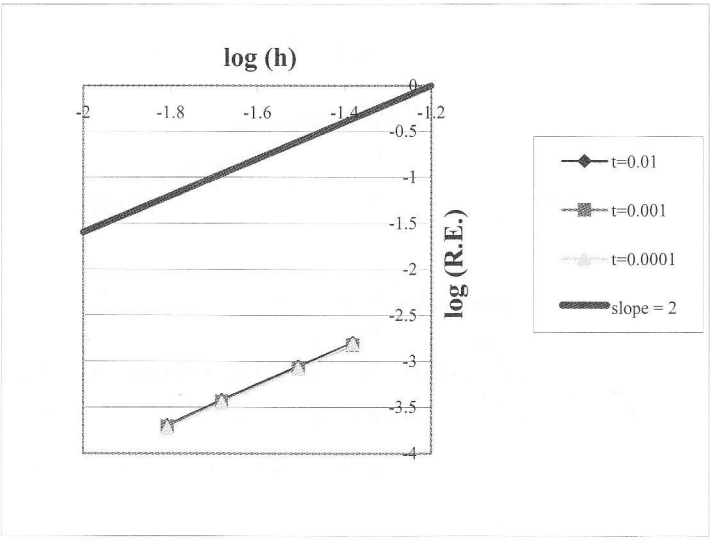

Figure 5. Convergence curves for the free hyperboloid shell modelled with graded meshes: we plot **log**(*R.E.*) where *R.E.* denotes the relative error $EM(u_{ref}, u_h) / A(u_{ref}, u_{ref})$ versus **log**(h).

3 On the solution of incompressible fluid flows – an FCBI scheme

In this section we first present the current state of a finite element solution approach that we are developing for high Reynolds number incompressible fluid flows and then describe some experiences with the procedure, see also [11]. We refer to the scheme as a flow-condition-based interpolation (FCBI) procedure.

3.1 Problem formulation and discretization

Let us consider, for ease of presentation, the solution of a planar two-dimensional problem of temperature-independent incompressible fluid flow. We assume that the fluid flow problem using the Navier-Stokes equations is well-posed in the Hilbert spaces V and P. The governing equations in conservative form are:

Find the velocity $\mathbf{v}(\mathbf{x},t) \in V$ and pressure $p(\mathbf{x},t) \in P$ such that

$$\frac{\partial \rho \mathbf{v}}{\partial t} + \nabla \cdot (\rho \mathbf{v}\mathbf{v} - \boldsymbol{\tau}) = \mathbf{0} \qquad (\mathbf{x},t) \in \Omega \times [0,T] \tag{11}$$

$$\nabla \cdot (\rho \mathbf{v}) = 0 \qquad (\mathbf{x},t) \in \Omega \times [0,T] \tag{12}$$

subject to the initial and boundary conditions

$$\mathbf{v}(\mathbf{x},0) = {}^0\mathbf{v}(\mathbf{x}), \qquad p(\mathbf{x},0) = {}^0p(\mathbf{x}) \qquad \mathbf{x} \in \Omega$$

$$\mathbf{v} = \mathbf{v}^s \qquad (\mathbf{x},t) \in \bar{S}_v \times (0,T] \tag{13}$$

$$\boldsymbol{\tau} \cdot \mathbf{n} = \mathbf{f}^s \qquad (\mathbf{x},t) \in S_f \times (0,T]$$

where

$$\boldsymbol{\tau} = \boldsymbol{\tau}(\mathbf{v},p) = -p\mathbf{I} + \mu\,[\,\nabla \mathbf{v} + (\nabla \mathbf{v})^T\,] \,. \tag{14}$$

Also, ρ is the density, μ is the viscosity, $\Omega \in R^2$ is a domain with the boundary $S = \bar{S}_v \cup S_f \;\; (S_v \cap S_f = \varnothing)$, T is the time span considered, $\mathbf{v}^s$ is the prescribed velocity on the boundary $\bar{S}_v$, $\mathbf{f}^s$ are the prescribed tractions on the boundary S_f and $\mathbf{n}$ is the unit normal to the boundary.

We note that the Navier-Stokes equations are self-consistent up to very high Reynolds numbers and weak solutions exist, provided of course transient analysis conditions are considered and the boundary and initial conditions are sufficiently smooth [22]. Hence, an "ideal" numerical solution scheme would have the following properties [10]:

--- The procedure would solve for the fluid flow at low and high Reynolds numbers even using rather coarse meshes. When the mesh is coarse, the solution would still be "overall" physically reasonably realistic.

--- The solution would be obtained using a Newton-Raphson iteration scheme that converges in a stable and fast manner.

--- As the mesh is refined, the same good convergence properties in the Newton-Raphson iterations are maintained and increasingly more detail in the flow is revealed.

--- As the mesh is refined, the convergence to the "exact" solution of the mathematical model would be optimal in convergence rate for the interpolation functions used.

--- These properties of numerical solution would hold even for very high Reynolds number flow, indeed also for conditions that would imply turbulence. Of course, when there are turbulent conditions, after the laminar solution has been calculated, in practice, a turbulence model would need to be used in order to obtain a physically meaningful/accurate solution.

This fluid flow "ideal" solution scheme does not yet exist, but it is reasonable to work towards the development of such a scheme. In the following we describe a 9-node FCBI element that we have developed in our research to obtain a procedure closer to the ideal solution scheme.

For the finite element solution, we use a Petrov-Galerkin variational formulation with subspaces V_h, U_h and W_h of V, and P_h and Q_h of P of the problem in Equations (11) through (14). The formulation used is:

Find $\mathbf{v} \in V_h$, $\mathbf{u} \in U_h$, $p \in P_h$ such that for all $w \in W_h$ and $q \in Q_h$

$$\int_{\Omega} w \left[\frac{\partial \rho \mathbf{u}}{\partial t} + \nabla \cdot (\rho \mathbf{u}\mathbf{v} - \boldsymbol{\tau}(\mathbf{u}, p)) \right] d\Omega = \mathbf{0} \tag{15}$$

$$\int_{\Omega} q \nabla \cdot (\rho \mathbf{u})\, d\Omega = 0 . \tag{16}$$

To define the spaces used in the formulation, consider Figure 6 where we show a mesh of elements in their natural coordinate systems. The figure shows a patch of typical 9-node elements and a "sub-element" which we use for the interpolation of the velocities. Each 9-node element is thought of to consist of four 4-node sub-elements.

The trial functions in U_h are defined as

$$\begin{bmatrix} h_1^u & h_4^u \\ h_2^u & h_3^u \end{bmatrix} = \mathbf{h}(\xi)\mathbf{h}^T(\eta) \tag{17}$$

where $\mathbf{h}^T(y) = [1-y, y]$ ($y = \xi, \eta$ with $0 \le \xi, \eta \le 1$). Similarly, an element in the space P_h is given by

$$\begin{bmatrix} h_1^p & h_4^p \\ h_2^p & h_3^p \end{bmatrix} = \mathbf{h}(r)\mathbf{h}^T(s) \ . \tag{18}$$

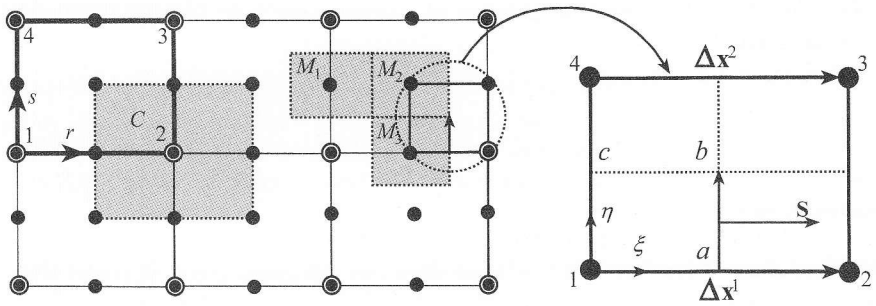

(a) 9-node elements (b) sub-element

Figure 6. A patch of 9-node elements. M_1, M_2, M_3 and C are typical control volumes for the nodes.

An important ingredient of the scheme is that the trial functions in V_h are defined using the flow conditions along each side of the sub-element. The functions are, for the flux through ab,

$$\begin{bmatrix} h_1^v & h_4^v \\ h_2^v & h_3^v \end{bmatrix} = \left[\mathbf{h}(x^1), \mathbf{h}(x^2)\right]\mathbf{h}(\eta)\mathbf{h}^T(\eta) \tag{19}$$

with

$$x^k = \frac{e^{q^k \xi} - 1}{e^{q^k} - 1}, \qquad q^k = \frac{\rho \, \bar{\mathbf{u}}^k \cdot \Delta \mathbf{x}^k}{\mu} \tag{20}$$

where $\bar{\mathbf{u}}^k \in U_h$ and is the velocity at the centre of the sides considered ($\xi = 1/2$ and $\eta = 0,1$ for $k = 1,2$ respectively). Analogous functions are used for the flux through bc and so on.

Finally, the elements in the space Q_h are step functions. Referring to Figure 6 we have, at node 2, for example,

$$h_2^q = \begin{cases} 1 & (r,s) \in [\frac{1}{2},1] \times [0,\frac{1}{2}] \\ 0 & \text{else} \end{cases} \tag{22}$$

Similarly, the weight functions in the space W_h are step functions, for example, at node 1,

$$h_1^w = \begin{cases} 1 & (\xi,\eta) \in [0,\frac{1}{2}] \times [0,\frac{1}{2}] \\ 0 & \text{else} \end{cases} \tag{23}$$

Note that the trial functions in U_h and V_h are "attached" to the same nodal velocities. The stability in the solution is obtained by use of the flow-condition-based functions in Equation (19) and the use of the weight functions in Equations (22) and (23). The use of the trial functions makes it possible to calculate consistent Jacobian matrices in the Newton-Raphson iterations to solve the finite element equations. Note that the step weight functions used in Q_h and W_h result in the use of control volumes around the finite element nodes. By use of these control volumes, conservation of mass and momentum is satisfied locally (and of course globally) in the finite element solution.

We demonstrate the solution scheme in some example solutions.

3.2 Example solutions using the FCBI procedure

We consider the S-channel flow problem shown in Figure 7. This problem is difficult to solve at higher Reynolds numbers because the corners in the geometry are forcing the flow to turn rapidly and a circulation exists in the horizontal exit section. We consider the flow at Re = 1, 100 and 10,000.

Figure 8 shows the two meshes used (coarse and fine) and the computed results for the velocities and pressures obtained with the 9-node element. We note that the meshes are rather coarse and yet reasonable flow solutions have been obtained. Of course, for a given coarse mesh, we must expect that the solution does not change significantly as we increase the Reynolds number beyond a certain value, which depends on the mesh.

We have also developed a 4-node FCBI finite element using in essence the same formulation. In this case, each node carries as unknowns the velocities and the pressure. Figure 9 shows the solutions to the problem using the same meshes with the 4-node element. Similar solution results as with the 9-node element are obtained. This element is particularly attractive because the matrices in the solutions have a much smaller bandwidth. Indeed, the equivalent 8-node three-dimensional FCBI element is effective for three-dimensional solutions (see Section 4).

Table 5 summarizes the number of Newton-Raphson iterations used in the solutions with the 4-node FCBI element. Here we note that the number of iterations somewhat increases with the Reynolds number and fineness of the mesh. As the mesh is

refined, more detail in the flow solution is predicted and this renders the solution more difficult.

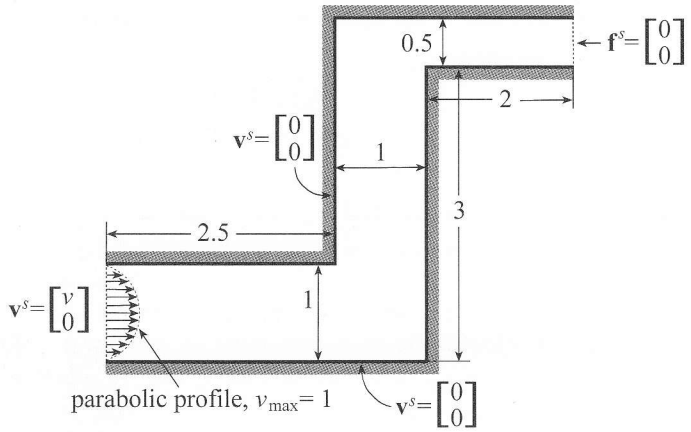

Figure 7. S-channel flow: problem definition.

4 On the solution of Navier-Stokes fluid flows fully coupled with structural interactions

There is now much interest in the solution of Navier-Stokes fluid flows fully coupled with structural interactions [2]. We have described the capabilities that we have researched and developed in references [12–17]. Briefly, the solution procedures can be used for fluid flows fully coupled to structures with the following modelling capabilities:

--- The linear or nonlinear structure is described by a Lagrangian formulation; the structural response can be highly nonlinear.

--- Contact and gap conditions can be included.

--- The fluid can be described by the incompressible (with or without heat transfer) Navier-Stokes equations.

--- The fluid can be described by the fully compressible Navier-Stokes equations for subsonic, transonic and supersonic flows.

--- The fluid flow can be modelled as laminar or turbulent flow.

--- An arbitrary-Lagrangian-Eulerian formulation is used for the fluid.

--- The mesh for the structure is usually completely independent, and different, from the mesh used for the fluid.

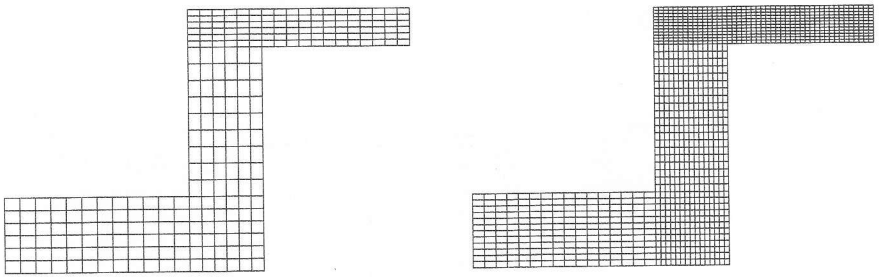

Figure 8a. Coarse and fine meshes employed in the analysis of the S-channel flow with the FCBI scheme (the same meshes are used with the 4-node and 9-node elements).

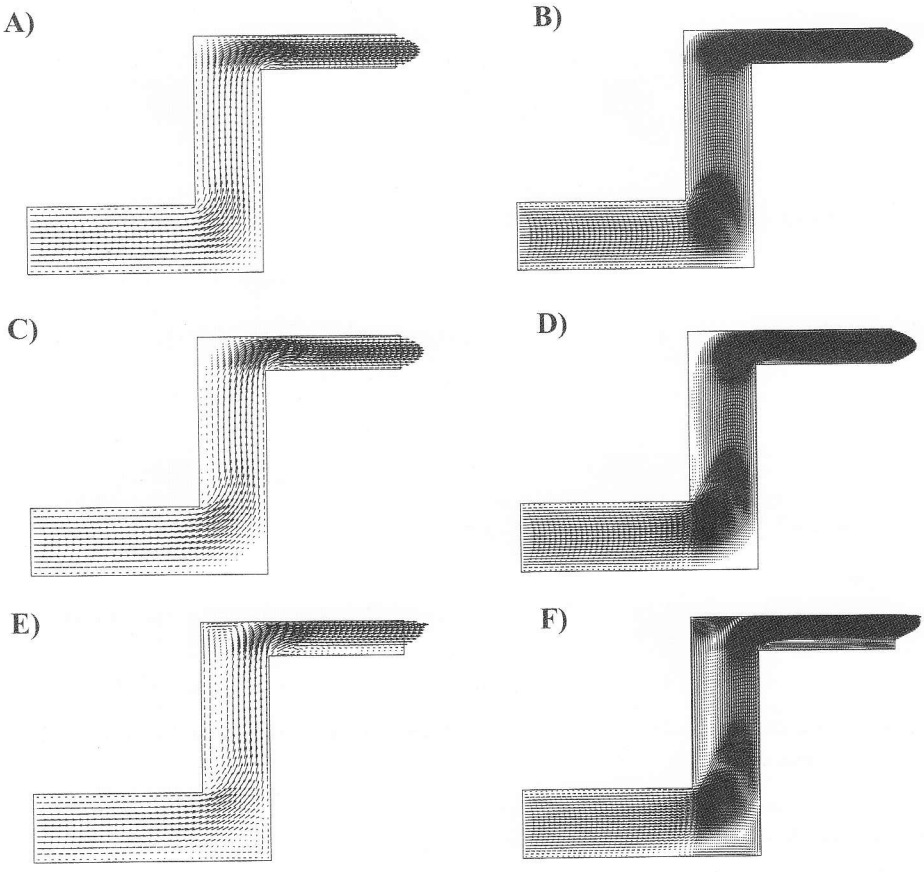

Figure 8b. S-channel flow: velocities computed with the 9-node FCBI element: A) Re=1, coarse mesh; B) Re=1, fine mesh; C) Re=100, coarse mesh; D) Re=100, fine mesh; E) Re=10,000, coarse mesh; F) Re=10,000, fine mesh.

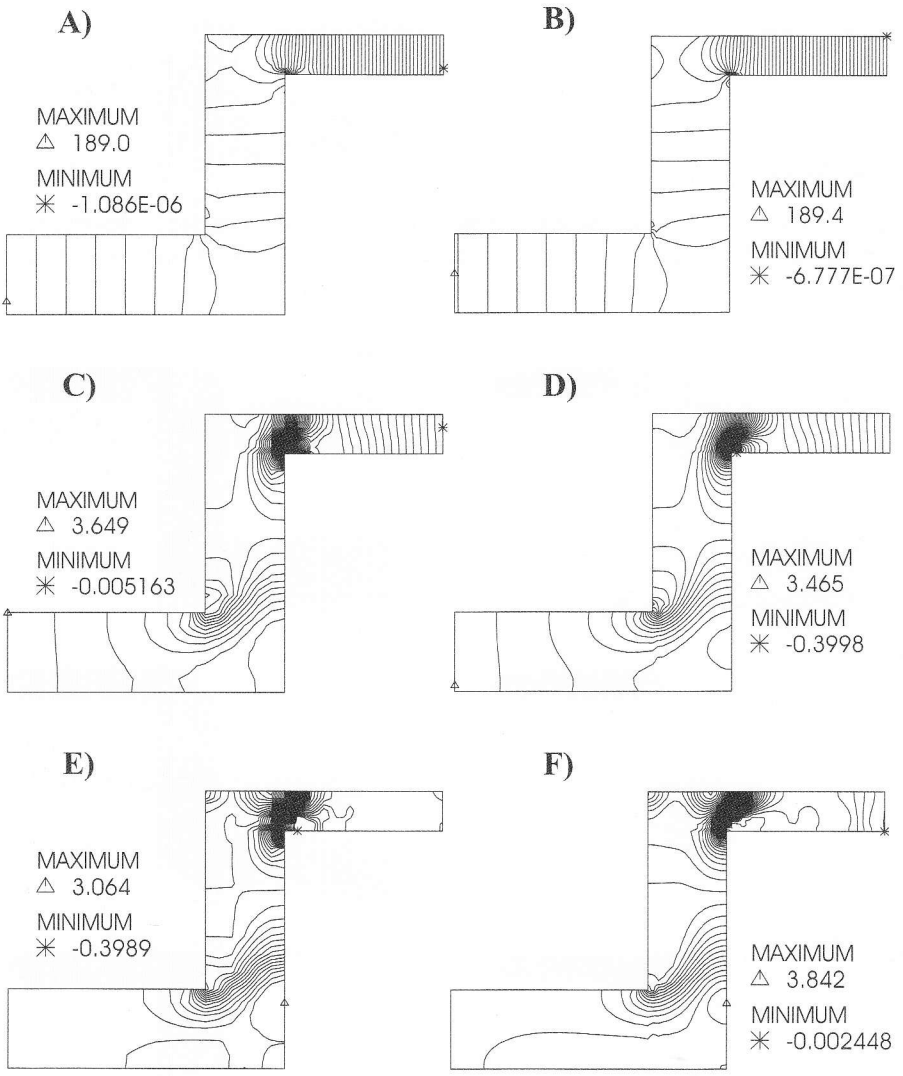

Figure 8c. S-channel flow: pressures computed with the 9-node FCBI element: A) Re=1, coarse mesh; B) Re=1, fine mesh; C) Re=100, coarse mesh; D) Re=100, fine mesh; E) Re=10,000, coarse mesh; F) Re=10,000, fine mesh.

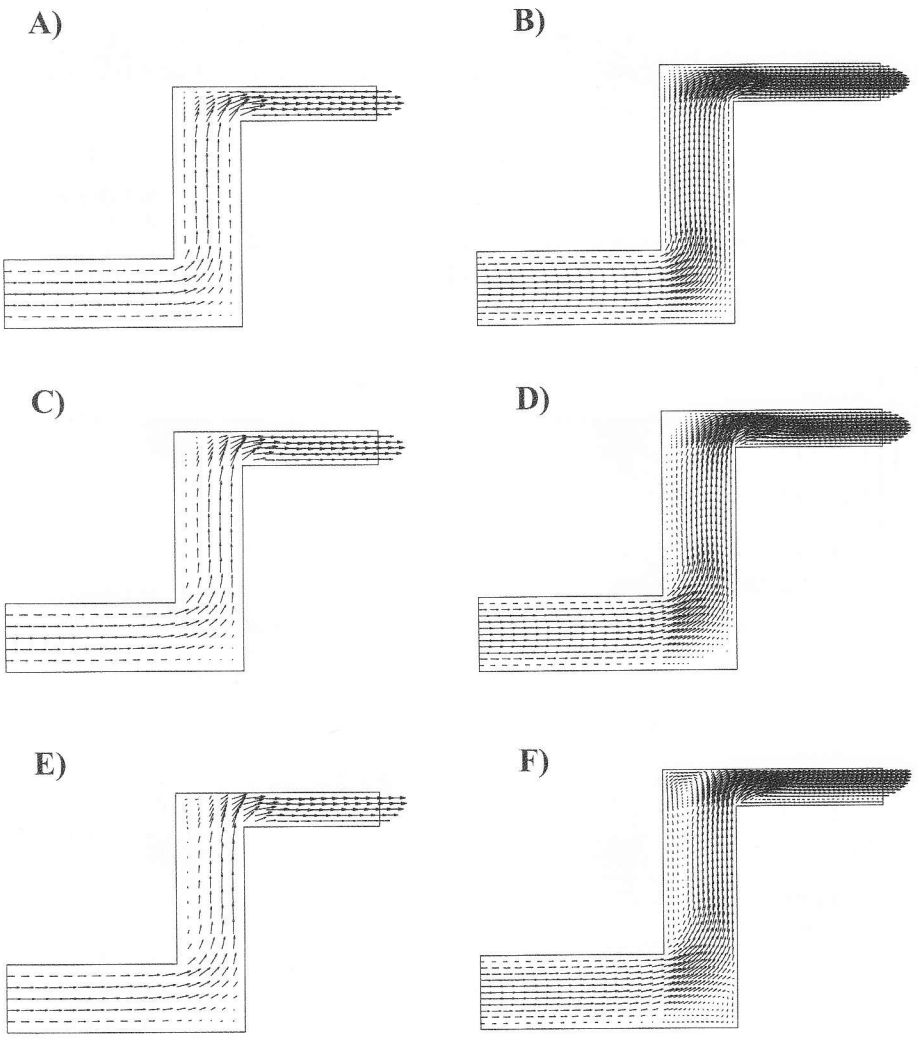

Figure 9a. S-channel flow: velocities computed with the 4-node FCBI element: A) Re=1, coarse mesh; B) Re=1, fine mesh; C) Re=100, coarse mesh; D) Re=100, fine mesh; E) Re=10,000, coarse mesh; F) Re=10,000, fine mesh.

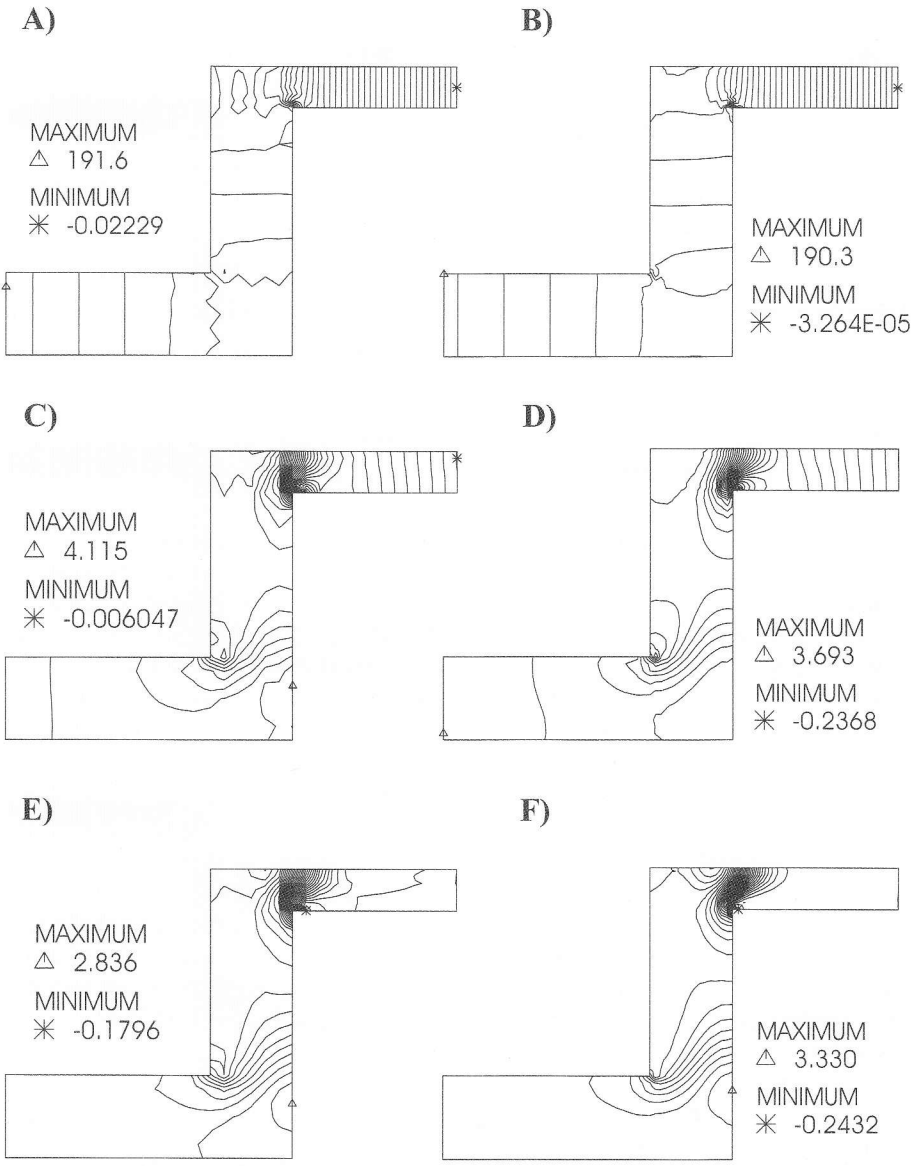

Figure 9b. S-channel flow: pressures computed with the 4-node FCBI element: A) Re=1, coarse mesh; B) Re=1, fine mesh; C) Re=100, coarse mesh; D) Re=100, fine mesh; E) Re=10,000, coarse mesh; F) Re=10,000, fine mesh.

Reynolds number	Mesh	Number of iterations
1	coarse	3
1	fine	3
100	coarse	4
100	fine	5
10,000	coarse	13
10,000	fine	24

Table 5. S-channel flow: number of Newton-Raphson iterations using the 4-node FCBI element. Convergence tolerance on the relative velocities is 10^{-5}.

At the same time as these capabilities have already been used widely, we of course have endeavoured to continuously increase the effectiveness of the solution techniques. This effectiveness is largely governed by the ability to obtain stable and accurate solutions in the arbitrary-Lagrangian-Eulerian formulation of the fluid flows. The ideal scheme for the solution of the fluid flow described above would clearly be a "key ingredient" in the overall solution procedure for the fluid-structural response. While the FCBI finite element solution procedure is not (yet) the ideal scheme, it is already an important ingredient to solve complex fluid flow structural interaction problems. We briefly present the solutions of two problems in the following.

The first solution is a rather simple demonstration of the capability. Figure 10 shows the analysis of a cantilever interacting with fluid flow in a channel. The meshes for the fluid and the cantilever are shown in Figure 10b. Note that completely different meshes are used for the cantilever and the fluid. We give the solutions for Re=100. The cantilever is subjected to very large displacements, shown to scale in Figures 10c and 10d.

In the second problem, we consider the fluid flow over a hemispherical thin shell, see Figure 11. This is a three-dimensional problem and we endeavour to use a rather coarse mesh for the fluid, even when high Reynolds number flow is considered, see Figure 11b. Figures 11c and 11d show the solutions obtained when the Reynolds number is equal to 100 and 10,000. The shell undergoes in both cases large displacements (to about 10 times its thickness). Clearly, a very coarse mesh has been used for the high Reynolds number fluid flow solution and accurate results cannot be expected. For an accurate solution a finer mesh would have to be used in further studies.

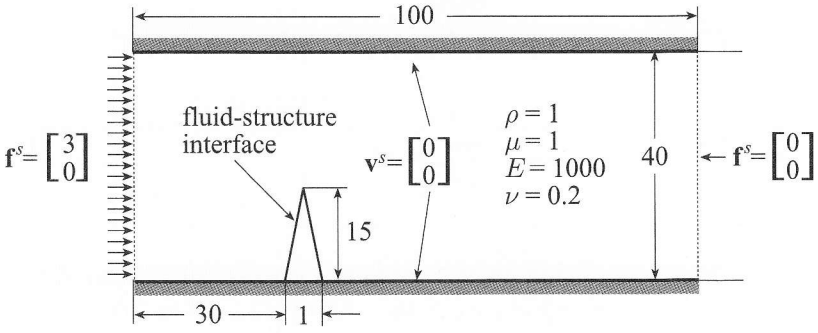

Figure 10a. Cantilever with fluid flow: problem definition.

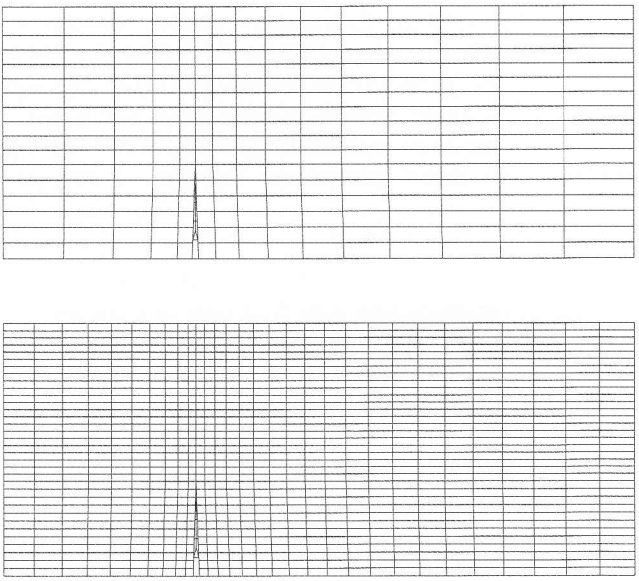

Figure 10b. Flow over a cantilever: coarse and fine meshes for the fluid and the same coarse mesh for the cantilever. 9-node solid elements for the cantilever and 9-node FCBI elements for the fluid.

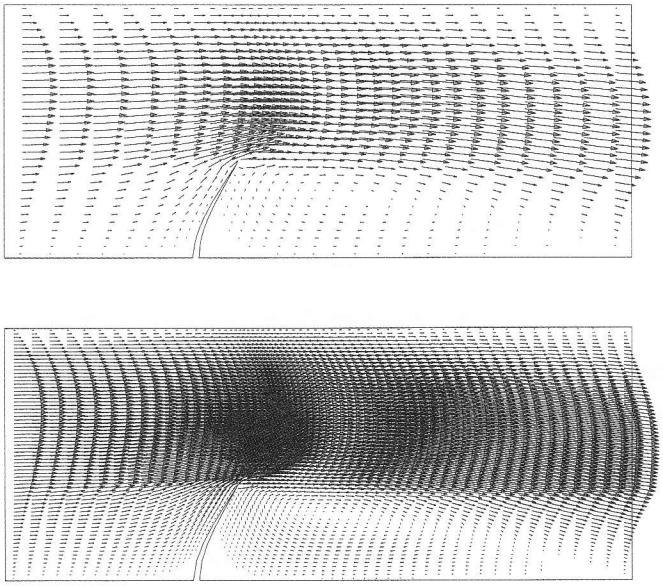

Figure 10c. Flow over a cantilever: velocities computed using the coarse mesh (top) and fine mesh (bottom) at Re = 100.

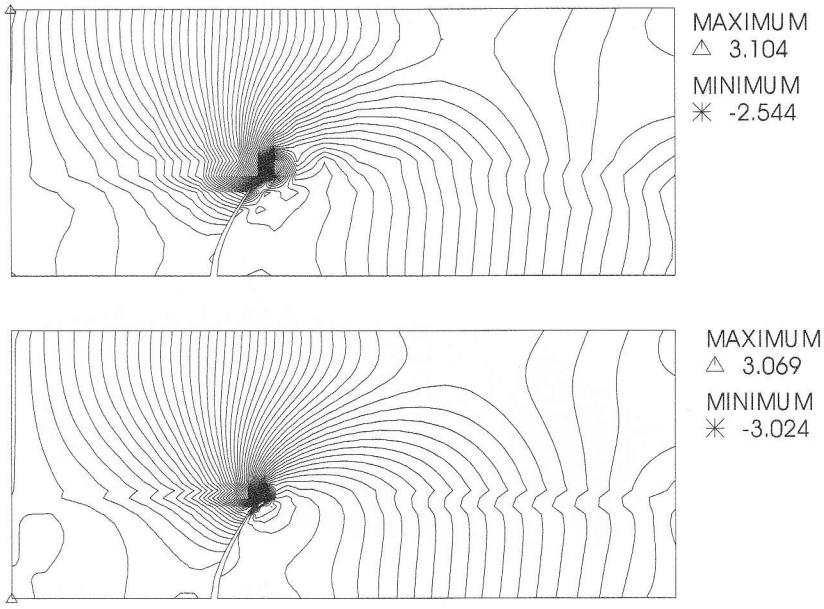

Fig 10d. Flow over a cantilever: pressures computed using the coarse mesh (top) and fine mesh (bottom) at Re = 100.

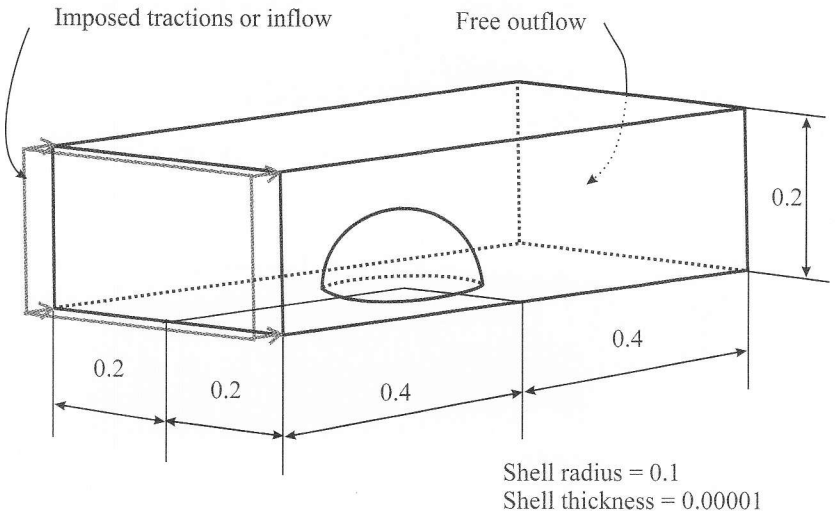

Figure 11a. Navier-Stokes fluid flow over a hemispherical thin shell: problem definition. No slip conditions are imposed on the bottom, top and sidewalls. For the case of Re=100, normal tractions are prescribed, and for the case of Re=10,000, the inflow velocity is prescribed.

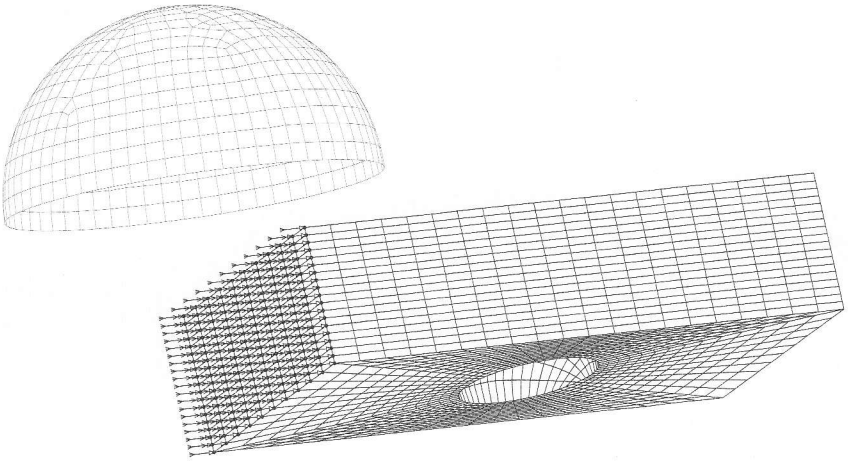

Figure 11b. Meshes for the shell and fluid (showing imposed velocities). MITC4 shell elements for the shell and 8-node FCBI elements for the fluid.

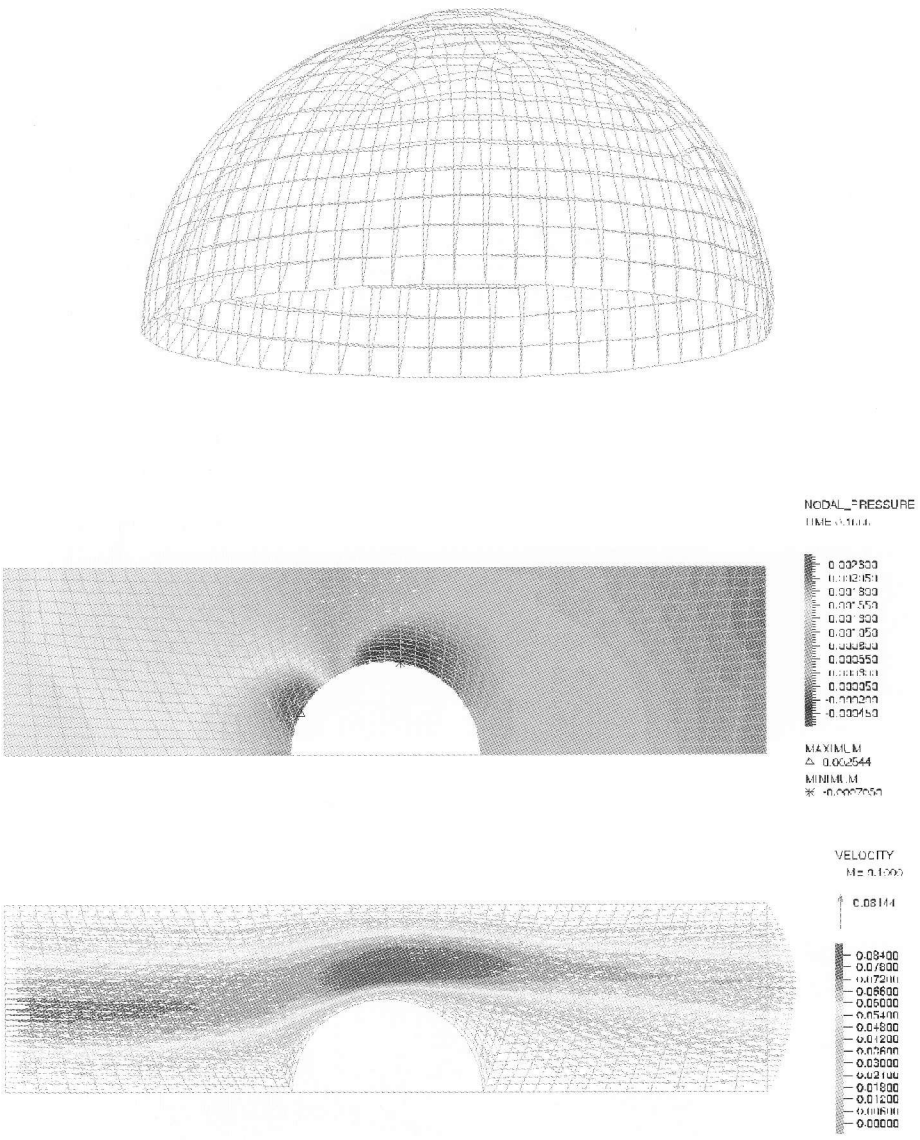

Figure 11c. Deformed geometry of the shell (top, deformations are enlarged), computed pressure distribution (middle) and computed velocity distribution (bottom) in the mid-plane for Re = 100.

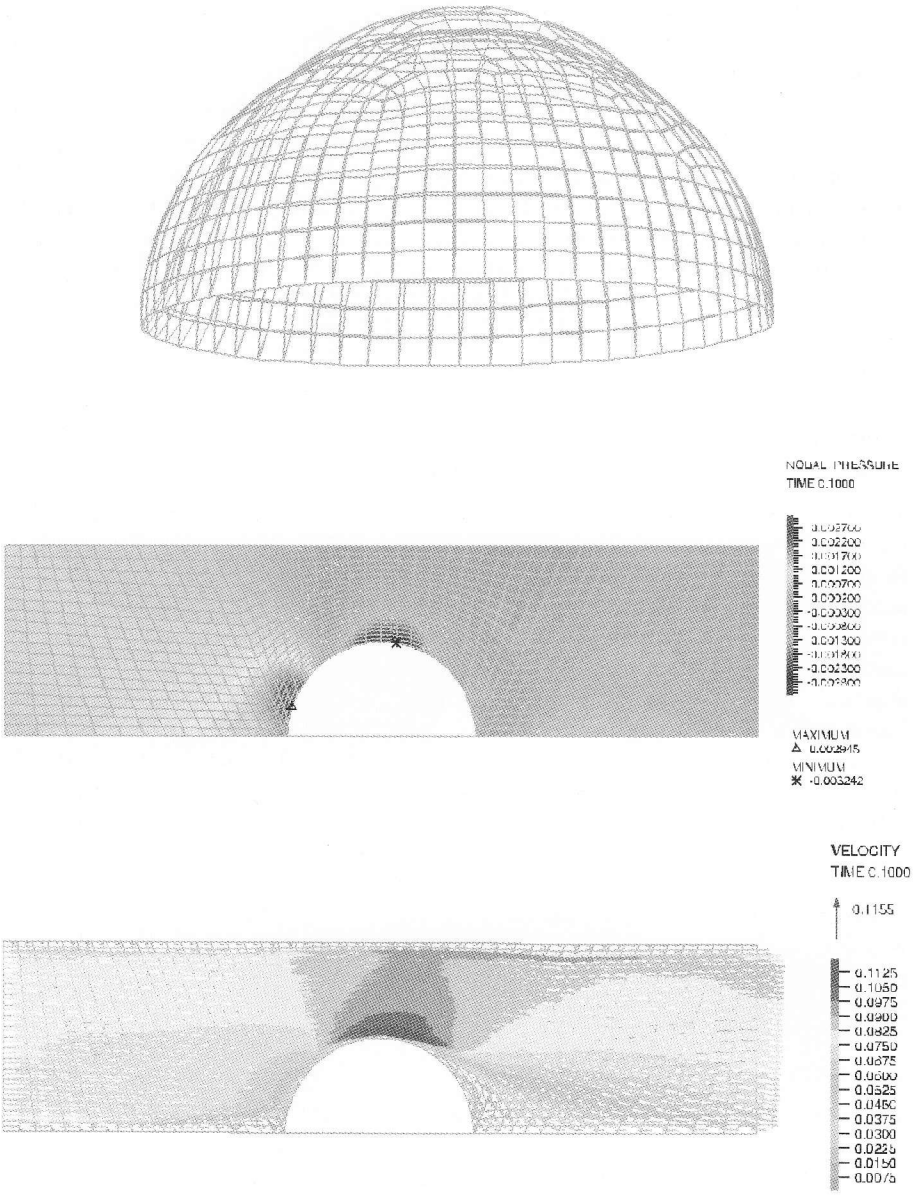

Figure 11d. Deformed geometry of the shell (top, deformations are enlarged), computed pressure distribution (middle) and computed velocity distribution (bottom) in the mid-plane for Re = 10,000.

5 Concluding remarks

The objective in this paper was to survey some of our latest research and development results in the analysis of shells, incompressible fluid flows and the full interaction between these flows and structures.

In the analysis of shells we have concentrated on gaining physical and mathematical insights into shell behaviours, in order to be able to establish effective procedures and benchmark problems for the evaluation of general finite element schemes. As discussed in the paper, it is very difficult to evaluate shell finite element methods thoroughly and comprehensively. Analytical investigations are largely out of reach and recourse must be taken to numerical investigations. These, of course, by their very nature, cannot be as comprehensive as analytical proofs but if properly designed can be of great value. We presented some of our thoughts in the paper and demonstrated our approach in some numerical studies.

With the mathematical understanding and numerical procedures available, a general foundation is in place to assess shell finite element methods quite thoroughly and design more effective discretization techniques.

Regarding the analysis of Navier-Stokes fluid flows, a major difficulty is that traditional numerical techniques frequently do not give solutions for flows at high Reynolds numbers when reasonable meshes are used, or require many iterations to reach converged solutions. We briefly described in the paper an "ideal" solution scheme and an FCBI finite element approach that we are developing to reach a method closer to this ideal technique. The key ingredients in this new finite element approach are that local mass and momentum conservation are satisfied and that interpolation functions based on the flow conditions are used. These functions are employed to reach stable solutions and to establish Jacobian matrices for the Newton-Raphson iterations. Some experiences with the so-far-developed solution scheme in this approach are presented in the paper. Of course, we endeavour to develop this FCBI procedure further in our continued research.

Considering fluid flow structural interaction problems, a flow solution scheme that is stable and reasonably accurate, even when using rather coarse meshes and considering high Reynolds number flows, is an important ingredient. In addition, the Newton-Raphson iteration scheme should be based on consistent Jacobian matrices for the fluid, the structure and the full coupling effects. We are developing the FCBI finite element scheme with these aims.

While of course many problems can already be solved with the existing finite element procedures, clearly, major improvements are still very desirable in the analysis techniques. This holds for the topics addressed in this paper, that is, the analysis of shells, fluid flows, and their coupled response, and many other areas of analysis. Eight key challenges regarding developments in finite element methods have been presented in reference [3], where it is also pointed out that these challenges will still provide much excitement in research and development for many years to come.

References

[1] Bathe, K.J., "Finite Element Procedures", Prentice Hall, 1996.
[2] Bathe, K.J., ed., "Computational Fluid and Solid Mechanics", Proceedings of the First M.I.T. Conference on Computational Fluid and Solid Mechanics, Elsevier, 2001.
[3] Bathe, K.J., "Key challenges at 40 years after", Proceedings of CUREE Symposium at UC Berkeley in honour of R.W. Clough and J. Penzien, May 2002.
[4] Chapelle, D., Bathe, K.J., "The Finite Element Analysis of Shells", Springer-Verlag, to appear.
[5] Chapelle, D., Bathe, K.J., "Fundamental considerations for the finite element analysis of shell structures", Computers and Structures, Vol. 66, pp. 19-36, 1998.
[6] Bathe, K.J., Iosilevich, A., Chapelle, D., "An evaluation of the MITC shell elements", Computers and Structures, Vol. 75, pp. 1-30, 2000.
[7] Bathe, K.J., Iosilevich, A., Chapelle, D., "An inf-sup test for shell finite elements", Computers and Structures, Vol. 75, pp. 439-456, 2000.
[8] Bathe, K.J., "The inf-sup condition and its evaluation for mixed finite element methods", Computers and Structures, Vol. 79, pp. 243-252, 971, 2001.
[9] Farshad M., "Design and Analysis of Shell Structures", Kluwer Academic Publishers, 1992.
[10] Hendriana, D., Bathe, K.J., "On upwind methods for parabolic finite elements in incompressible flows", Int. J. Num. Meth. in Eng., Vol. 47, pp. 317-340, 2000.
[11] Bathe, K.J., Zhang, H., "A flow-condition-based interpolation finite element procedure for incompressible fluid flows", Computers and Structures, in press.
[12] Bathe, K.J., Zhang, H., Wang, M.H., "Finite element analysis of incompressible and compressible fluid flows with free surfaces and structural interactions", Computers and Structures, Vol. 57, pp. 193 – 213, 1995.
[13] Bathe, K.J., "Simulation of structural and fluid flow response in engineering practice", Computer Modeling and Simulation in Engineering, Vol. 1, pp. 47 - 77, 1996.
[14] Bathe, K.J., Zhang, H., Zhang, X., "Some advances in the analysis of fluid flows", Computers and Structures, Vol. 64, pp. 909-930, 1997.
[15] Bathe, K.J., Zhang, H., Ji, S., "Finite element analysis of fluid flows fully coupled with structural interactions", Computers and Structures, Vol. 72, pp. 1-16, 1999.
[16] Rugonyi, S., Bathe, K.J., "On the finite element analysis of fluid flows fully coupled with structural interactions", Computer Modeling in Engineering and Sciences, Vol. 2, pp. 195-212, 2001.
[17] Zhang, H., Bathe, K.J., "Direct and iterative computing of fluid flows fully coupled with structures", Computational Fluid and Solid Mechanics (K.J. Bathe, ed.), pp. 1440-1443, Elsevier, 2001.
[18] Sanchez-Hubert, J., Sanchez-Palencia, E., "Coques Elastiques Minces – Propriétés Asymptotiques", Masson, Paris.

[19] Lee, P.S., Bathe, K.J., "On the asymptotic behavior of shell structures and the evaluation in finite element solutions", Computers and Structures, Vol. 80, pp. 235-255, 2002.

[20] Bathe, K.J., Chapelle, D., Lee, P.S., "A shell problem 'highly-sensitive' to thickness changes", Int. J. Num Meth. in Eng., submitted.

[21] Hiller, J.F., Bathe, K.J., "On the assessment of mixed finite element formulations with special reference to shell discretization schemes", in preparation.

[22] Foias, C., Manley, O., Rosa, R., Temam, R., "Navier-Stokes Equations and Turbulence", Cambridge University Press, 2001.